Water Oxidation

DOI: 10.1002/ange.201306585

Optically Transparent Water Oxidation Catalysts Based on Copper Nanowires**

*Zuofeng Chen, Aaron R. Rathmell, Shengrong Ye, Adria R. Wilson, and Benjamin J. Wiley**

Water oxidation ($2H_2O \rightarrow O_2 + 4e^- + 4H^+$) is a key step for converting solar energy into chemical fuels.[1,2] Nickel and cobalt oxides are appealing anode materials for water oxidation because of their abundance and high catalytic activity at neutral to basic solution conditions.[3–11] These oxides are typically electrodeposited on an indium tin oxide (ITO) substrate for use in photoelectrosynthesis cells (PECs).[12,13] ITO is used because of its high transmittance (ca. 90% in the visible spectrum) at low sheet resistances (10–15 $\Omega\,sq^{-1}$).[14,15] However, the instability of ITO surfaces at the high anodic potentials required for water oxidation can lead to a loss of conductivity.[16,17] Indium is a scarce element, and the vapor-phase sputtering process used to make ITO films further contributes to their high cost.[15] The light blocked by nickel and cobalt oxide catalyst films can also decrease the light harvesting efficiency of the dye or photovoltaic component of a PEC.[11,12]

Herein we report a new approach to create transparent catalysts for water oxidation that eliminates the need for ITO. We replaced the ITO electrode with a conducting network of copper nanowires (Cu NWs), which have the advantage of being made from an element that is 1000 times more abundent and 100 times less expensive than indium, and can be deposited using fast liquid-phase coating processes.[18–21] We then use electrodesposition to create a conformal layer of nickel or cobalt around the NWs to serve as a catalyst. These core–shell NW networks exhibit sustained electrocatalytic water oxidation with activities comparable to thin films of metal oxides, but transmit up to 6.7 times more light.

Cu NWs (>20 μm in length and ca. 70 ± 25 nm in diameter) were synthesized and coated onto glass by following procedures reported previously (see the Supporting Information).[22,23] The Cu NW film (65 $mg\,m^{-2}$) exhibited a sheet resistance of 32 $\Omega\,sq^{-1}$ at a transmittance of 85% ($\lambda = 550$ nm; all of the transmittance values refer to specular transmittance). The transmittance and sheet resistance of a NW film can be varied by simply changing the areal density of the NWs.[22] A comparison of the performance of Cu NW films with ITO and other alternatives has been reported.[22,23]

We have previously demonstrated the electroless plating of Ni onto Cu NWs dispersed in ethylene glycol at 120°C prior to film formation.[23] Here, we chose to electroplate Ni onto Cu NWs after film formation because it avoids laborious centrifugation and washing steps, eliminates ethylene glycol waste, can be carried out at room temperature, and prevents the aggregation of NWs due to the magnetic attraction beween Cu-Ni NWs. Electroplating has the additional benefits of being more controllable, reproducible, and versatile (applicable to a wider range of metals) than electroless plating.

The Cu NW network was coated with Ni by electroplating Ni^{II} onto the network in deaerated borate buffer (pH 9.2) at room temperature. As shown in Figure 1A, the cyclic voltammetry (CV) profile of the Cu NW network in solution without Ni^{II} is relatively featureless. The double-layer charging current is 80% that of a polycrystalline copper foil of the same geometric surface area (Supporting Information, Figure S1A), even though the fractional area coverage of the Cu NWs on the glass is 0.13.[24] Upon addition of 0.5 mM $NiCl_2$, the CV exhibits a redox couple consistent with $Ni^{II} + 2e^- \rightarrow Ni^0$ (−0.25 V vs. NHE).

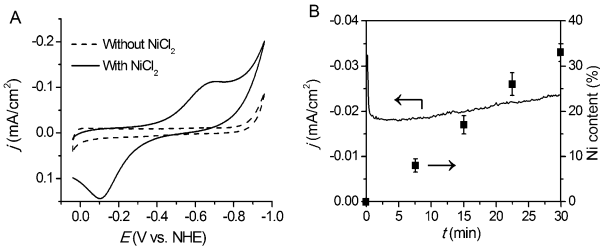

Figure 1. A) Cyclic voltammograms of a Cu NW network in 0.2 M deaerated borate buffer (pH 9.2) with and without 0.5 mM $NiCl_2$ added to the solution. Scan rate 100 $mV\,s^{-1}$. B) Current and Ni content of the film as a function of time during electroplating at −0.75 V vs. NHE.

Continuous electroplating was conducted by holding the potential at −0.75 V vs. NHE for 30 min (Figure 1B). Both the transmittance and the sheet resistance of the NW network decreased slightly as the thickness of the nickel coating increased (Supporting Information, Figure S2). The Cu-Ni core–shell (Cu_c-Ni_s) NW network produced by the electrodeposition shown in Figure 1B contained 33 wt% Ni, exhibited a transmittance of 80% at 550 nm, and had a sheet resistance of 26 $\Omega\,sq^{-1}$. These transmittance and sheet resistance values are equivalent to those obtained by using electroless deposition, as was the stability of the films when stored in an oven at 85°C (Supporting Information, Fig-

[*] Dr. Z. Chen, Dr. A. R. Rathmell, Dr. S. Ye, A. R. Wilson, Prof. B. J. Wiley
Department of Chemistry, Duke University
Durham, NC 27708 (USA)
E-mail: benjamin.wiley@duke.edu

[**] This work was supported in part by the NSF Research Triangle MRSEC (DMR-1121107) and an NSF CAREER award (DMR-1253534). A.R.W. was supported by a NSF graduate research fellowship.

Supporting information for this article is available on the WWW under http://dx.doi.org/10.1002/anie.201306585.

ure S3).[23] This percentage of Ni is close to the minimum necessary to obtain complete coverage of the surface of the Cu NWs and prevent their oxidation.

Dark-field optical microscopy (DFOM) images (Figure 2 A and B) demonstrate that the Cu NWs are evenly dispersed across the glass substrate and are interconnected.

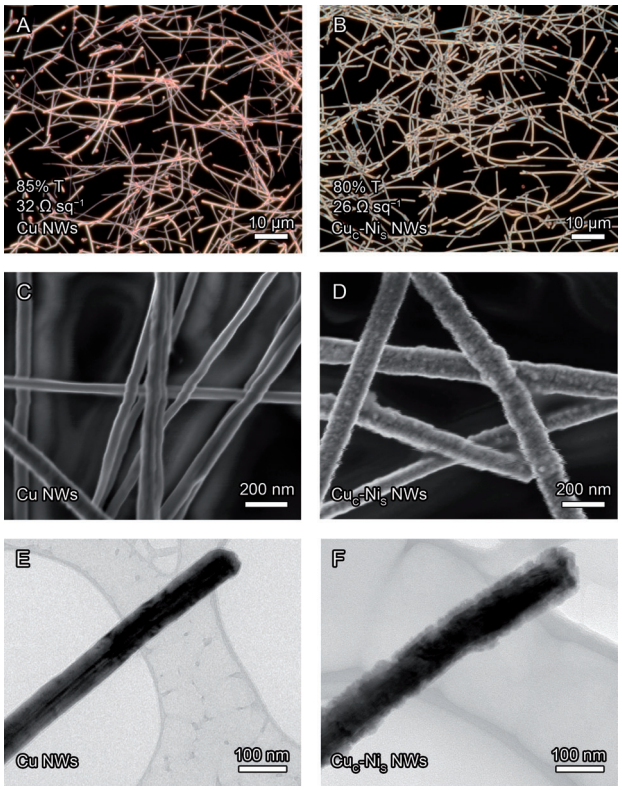

Figure 2. Dark-field optical microscopy (A,B), SEM (C,D), and TEM (E,F) images of Cu NWs (A,C,E) and Cu$_c$-Ni$_s$ NWs (B,D,F) formed by the electroplating process shown in Figure 1 B.

The color of light scattered from the NWs changes from reddish-orange to neutral gray upon coating with 33 wt% nickel. The electroplating of Ni occured only on the surface of the Cu NWs, with no nickel deposited on the open areas of the substrate. This allowed the network to retain its transmittance after electroplating. Furthermore, Ni electroplating occured only at electrically connected Cu NWs. In a control experiment on a film comprised of a less dense network of Cu NWs (90% transmittance at 550 nm, 170 Ω sq^{-1}), the occasional isolated Cu NW remained uncoated and reddish-orange in color (Supporting Information, Figure S4).

The SEM images in Figure 2 C and D show that the surface roughness of the NWs increased after Ni coating and the diameter of the NWs increased from 70 ± 25 nm to 95 ± 30 nm. The double-layer charging current of the Cu$_c$-Ni$_s$ film is about 1.3 times that of a polycrystalline Ni foil of the same geometric surface area (Supporting Information, Figure S1B). The electroplating rate could be accelerated by holding the film at more negative potentials (for example, −0.80 V or −0.85 V), but electroplating at these potentials increased the roughness of the nickel layer (Supporting Information, Figure S5). Figure 2 E and F show TEM images of the Cu$_c$-Ni$_s$ NWs in which the core–shell structure is visible.

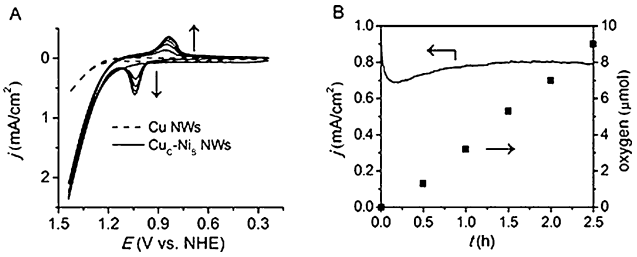

Figure 3. A) Cyclic voltammograms of Cu NW and Cu$_c$-Ni$_s$ NW networks (33 wt% Ni) in 0.2 M borate buffer (pH 9.2). Scan rate 100 mV s^{-1}. The arrow indicates the current peaks increase with scan cycles. B) Constant potential electrolysis with a Cu$_c$-Ni$_s$ NW network (33 wt% Ni) at 1.30 V vs. NHE with 0.03 mM Ni(NO$_3$)$_2$ added to the solution.

The thickness of this rough shell was determined to be 13 ± 5 nm from the TEM images.

Figure 3 A shows CVs obtained for Cu NW and Cu$_c$-Ni$_s$ (33% Ni) NW film electrodes in 0.2 M aqueous borate buffer (pH 9.2). In the absence of a Ni coating, only a relatively small background oxygen evolution occurs at about 1.30 V. After Ni coating, the current from water oxidation increased dramatically on the first anodic scan with an onset potential at about 1.15 V, below which there were no distinct redox peaks. The cathodic return scan exhibited a broad feature at about 0.84 V, which we attribute to the reduction of a higher oxidation state Ni species formed during the initial sweep through the catalytic wave. Subsequent CV scans displayed a sharp anodic prefeature centered at about 1.05 V. The anodic and the cathodic prefeatures gradually increased in amplitude with continued scanning.

The Cu$_c$-Ni$_s$ NW film electrode was also used for constant potential electrolysis at 1.30 V vs. NHE in the presence of 0.03 mM Ni(NO$_3$)$_2$ and aqueous borate buffer (pH 9.2). Addition of dilute Ni^{II} is essential for sustained long-term electrolysis. With no Ni^{II} ions added to the solution, the coated Ni layer gradually dissolved by oxidation after prolonged electrolysis. A self-repair mechanism was proposed to explain the sustained electrocatalytic water oxidation by NiO_xH_y or CoO_xH_y clusters and/or films formed in situ from added Ni^{II} or Co^{II}.[3,4] Figure 3 B shows that over the first 10 min of electrolysis, the current dropped about 25%, after which the current increased, which is presumably due to the activation of the coated Ni layer and compensatory anodic deposition of Ni^{II} ions. Catalysis was sustained at a geometric current density of about 0.80 mA cm^{-2}. Based on the ratio of the double layer charging current between this NW film and a polycrystalline nickel foil of the same surface area, the current desntiy per surface area of the NWs is 0.6 mA cm^{-2}. Figure 3 B shows that about 9.0 μmol of O_2 was produced over a period of 2.5 h, with a Faradaic efficiency of 95%.

As shown in Figure 4 A, a catalytic current density of 1.40 mA cm^{-2} could be achieved under identical experimental conditions by increasing the density of Cu NWs to about 100 mg m^{-2}. After compensating for the *iR* drop from the solution, we obtained an activity of 1 mA cm^{-2} at an overpotential of about 440 mV for the 100 mg m^{-2} film. This is comparable to an activity of 1 mA cm^{-2} at an overpotential of

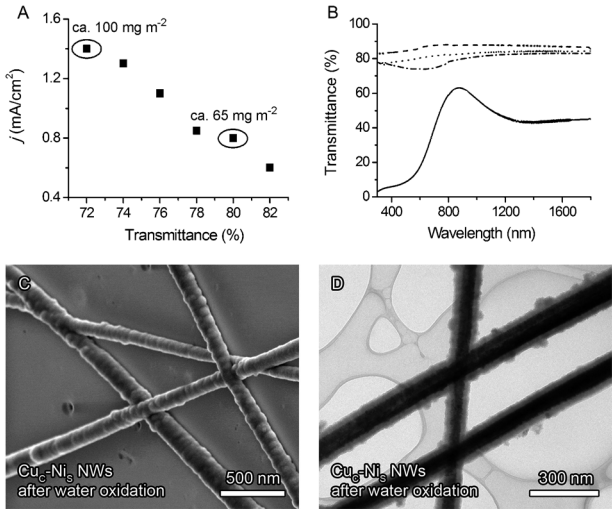

Figure 4. A) A plot of the transmittance of Cu_c-Ni_s NW networks versus catalytic current density of water oxidation. B) Plots of transmittance versus wavelength for films of Cu NWs (-----), Cu_c-Ni_s NWs (•••••), and Cu_c-Ni_s NWs (–•–•) after sustained water oxidation, and a NiO_xH_y cluster film on ITO (——) formed from anodic deposition of Ni^{II} ions. C) SEM and D) TEM images of Cu_c-Ni_s NW networks after water oxidation.

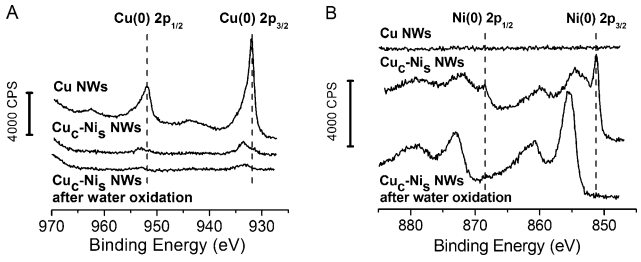

Figure 5. XPS spectra of the A) Cu and B) Ni species present on Cu NW, Cu_c-Ni_s NW, and Cu_c-Ni_s NW networks after water oxidation. CPS = counts per second.

about 425 mV for an electrodeposited NiO_xH_y cluster film on ITO under the same pH.[4] The trend in Figure 4A suggests an even higher catalytic current density can be attained at the expense of film transmittance.

To compare the transmittance of the NW films with a benchmark, we followed previously published procedures to prepare an electrodeposited NiO_xH_y cluster film on ITO that gave the same geometric current density (ca. 0.8 mA cm^{-2}) as a Cu_c-Ni_s network (65 mg m^{-2} Cu NWs).[4–6] Figure 4B shows the transmittance of the Cu_c-Ni_s NW film at $\lambda = 550$ nm drops from 80% to 74% after the water oxidation. The SEM image in Figure 4C shows that the network appeared well-preserved after water oxidation, with no observable deposition of solid precipitate in the open areas of the film. The TEM image in Figure 4D shows that the core–shell structure of the NW became more distinct after water oxidation owing to an increase in the thickness of the Ni shell from 13 ± 5 nm to 28 ± 8 nm. This increase in the shell thickness accounts for the decrease in the transmittance of the network film after water oxidation, and is most likely due to the anodic deposition of Ni^{II} ions onto the NWs. Despite the slight decrease in transmittance after water oxidation, the transmittance of the NW network film is still approximately 6.7 times more tranparent (74% at $\lambda = 550$ nm) than the NiO_xH_y cluster film on ITO (11%) of the same activity. Averaging over the wavelengths of 300–1800 nm, the transmittance of the Cu_c-Ni_s NW film is 80.2% versus 39.3% for the NiO_xH_y cluster film on ITO.

We performed X-ray photoelectron spectroscopy (XPS) on the NWs to further characterize their compositional changes after electrodeposition and water oxidation. XPS of Cu NWs (Figure 5A) exhibits peaks at 932.0 and 951.8 eV, which are characteristic of the $2p_{3/2}$ and $2p_{1/2}$ binding energies of Cu(0) metal.[25] The small rounded peaks at 943.6 and 962.4 eV can be attritubed to CuO[25] on the surface of the Cu NWs. After coating the Cu NWs with Ni, the signal for Cu almost disappeared (Figure 5A), and peaks for the $2p_{3/2}$ and $2p_{1/2}$ binding energies of Ni^0 appeared at 851.3 and 868.7 eV,[25,26] respectively (Figure 5B). Additional peaks also formed at 853.9, 860.1, 871.8, and 879.0 eV after nickel deposition. These peaks have previously been assigned to NiO.[25,26] After water oxidation, the Ni^0 peaks disappeared and those originally assigned to NiO intensified and shifted toward higher binding energies. The $2p_{3/2}$ and $2p_{1/2}$ peak at 853.9 eV and 871.8 eV shifted to 855.3 eV and 873.3 eV, respectively, which is most likely due to the formation of $Ni(OH)_2$ and/or NiOOH during water oxdation.[5,6,25,26]

As shown in the Supporting Information, Figures S6 and S7, the electroplating of Ni on the Cu NW network and the activity of the Cu_c-Ni_s NW network toward water oxidation was not altered by the replacement of glass with flexible polyethylene terephthalate (PET). Figure 6 shows that a film

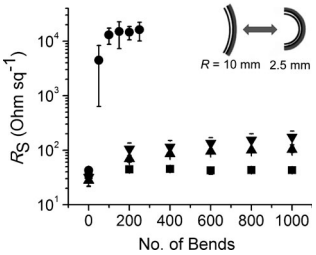

Figure 6. Plots of sheet resistance (R_S) versus number of bends for ITO film (●), Cu NW film (■), Cu_c-Ni_s NW film (33 wt% Ni; ▲), and Cu_c-Ni_s NW film (33 wt% Ni) after water oxidation (▼) on PET.

of Cu_c-Ni_s NW (33 wt% Ni) on PET exhibited a relatively small increase in sheet resistance from 28 to 103 Ω sq^{-1} after 1000 bends, and this flexibility is retained after water oxidation. This is in contrast to ITO on PET, for which the sheet resistance increased by 400 times after just 250 bends. The relatively greater flexibility and mechanial durability of nanowire films may expand the design space for PECs.[16,17]

To demonstrate the versatility of electroplating on Cu NW networks as a way to make transparent electrocatalysts, we also fabricated a Cu_c-Co_s NW film and used it for water oxidation. The Cu NW network (85% at 550 nm, 32 Ω sq^{-1}) was coated with Co by electroplating Co^{II} onto the network in a deaerated phosphate buffer (pH 7.0) at room temperature. A CV (Supporting Information, Figure S8A) shows a redox

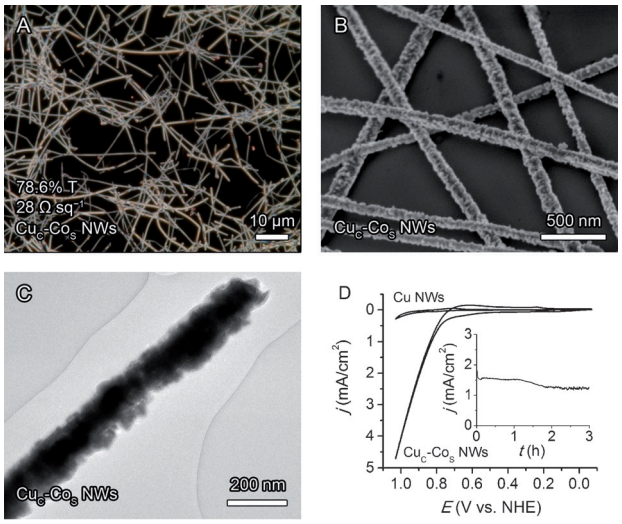

Figure 7. A) Dark-field optical microscopy, B) SEM, and C) TEM images of Cu_c-Co_s NW networks (40 wt% Co) made by electroplating (See the Supporting Information, Figure S8B). D) Cyclic voltammograms of Cu NW and Cu_c-Co_s NW networks (40 wt% Co) in 1 M NaOH. Scan rate 100 mV s^{-1}. Inset: constant potential electrolysis with a Cu_c-Co_s NW network (40 wt% Co) at 0.86 V vs. NHE with 0.1 mM added $Co(ClO_4)_2$.

couple corresponding to $Co^{II} + 2e^- \leftrightarrow Co^0$ (−0.28 V vs. NHE). Continuous electroplating was conducted by holding the potential at −0.75 V vs. NHE for 20 min (Supporting Information, Figure S8B), resulting in a Cu_c-Co_s NW network with a cobalt content of about 40 wt%, a transmittance of 78.6% at 550 nm, and a sheet resistance of 26 Ω sq^{-1}.

Figure 7 A–C shows optical, SEM, and TEM images of the Cu_c-Co_s NW network. The images appear similar to the Cu_c-Ni_s NW network with the exception that the Co layer is more rough than the nickel layer. From the TEM image in Figure 7 C, the thickness of the Co shell was estimated to be 15 ± 7 nm. Figure 7 D shows the Cu_c-Co_s NW network exhibits a pre-wave couple at about 0.25 V followed by catalytic current onset at about 0.71 V in 1 M NaOH. The Cu_c-Co_s NW network exhibited sustained electrocatalytic water oxidation of 1.35 mA cm^{-2} at 0.86 V vs. NHE, with an overpotential of 425 mV after compensating for the solution *iR* drop. The NW film maintained a transmittance of about 77% at 550 nm over the course of water oxidation. As with the Cu_c-Ni_s NW network, higher catalytic current densities can be attained for the Cu_c-Co_s NW network by increasing the areal density of NWs at the expense of film transmittance.

We have demonstrated that networks of Cu-Ni and Cu-Co core–shell nanowires can be fabricated by deposition of solution-synthesized Cu nanowires, followed by electrodeposition. This fabrication method can most likely be extended to create core–shell nanowire networks with a wide variety of compositions for various applications. Core–shell nanowire networks exhibit electrocatalytic performance for water oxidation equivelant to metal oxide films of similar composition, but are several times more transparent. The greater transmittance, mechancial flexibility, and lower materials cost of nanowire network catalysts relative to thin film catalysts deposited on ITO opens up new possibilities to engineer more efficient, mechanically robutst, and affordable light-harvesting architectures for scalable production of solar fuels.[12]

Received: July 28, 2013
Revised: September 18, 2013
Published online: October 18, 2013

Keywords: copper · nanowires · nickel · transparent electrodes · water oxidation

[1] T. R. Cook, D. K. Dogutan, S. Y. Reece, Y. Surendranath, T. S. Teets, D. G. Nocera, *Chem. Rev.* **2010**, *110*, 6474 – 6502.
[2] M. G. Walter, E. L. Warren, J. R. McKone, S. W. Boettcher, Q. Mi, E. A. Santori, N. S. Lewis, *Chem. Rev.* **2010**, *110*, 6446 – 6473.
[3] M. W. Kanan, D. G. Nocera, *Science* **2008**, *321*, 1072 – 1075.
[4] M. Dincă, Y. Surendranath, D. G. Nocera, *Proc. Natl. Acad. Sci. USA* **2010**, *107*, 10337 – 10341.
[5] D. K. Bediako, B. Lassalle-Kaiser, Y. Surendranath, J. Yano, V. K. Yachandra, D. G. Nocera, *J. Am. Chem. Soc.* **2012**, *134*, 6801 – 6809.
[6] M. Risch, K. Klingan, J. Heidkamp, D. Ehrenberg, P. Chernev, I. Zaharieva, H. Dau, *Chem. Commun.* **2011**, *47*, 11912 – 11914.
[7] L. Trotochaud, J. K. Ranney, K. N. Williams, S. W. Boettcher, *J. Am. Chem. Soc.* **2012**, *134*, 17253 – 17261.
[8] G. Zhu, E. N. Glass, C. Zhao, H. Lv, J. W. Vickers, Y. V. Geletii, D. G. Musaev, J. Song, C. L. Hill, *Dalton Trans.* **2012**, *41*, 13043 – 13049.
[9] J. B. Gerken, J. G. McAlpin, J. Y. C. Chen, M. L. Rigsby, W. H. Casey, R. D. Britt, S. S. Stahl, *J. Am. Chem. Soc.* **2011**, *133*, 14431 – 14442.
[10] F. Jiao, H. Frei, *Angew. Chem.* **2009**, *121*, 1873 – 1876; *Angew. Chem. Int. Ed.* **2009**, *48*, 1841 – 1844.
[11] T. Zidki, L. Zhang, V. Shafirovich, S. V. Lymar, *J. Am. Chem. Soc.* **2012**, *134*, 14275 – 14278.
[12] S. Y. Reece, J. A. Hamel, K. Sung, T. D. Jarvi, A. J. Esswein, J. J. H. Pijpers, D. G. Nocera, *Science* **2011**, *334*, 645 – 648.
[13] D. Gust, T. A. Moore, A. L. Moore, *Acc. Chem. Res.* **2009**, *42*, 1890 – 1898.
[14] R. G. Gordon, *MRS Bull.* **2000**, *25*, 52 – 57.
[15] U.S. Geological Survey, Mineral Commodity Summaries. Indium, **2011**, 74.
[16] G. Folcher, H. Cachet, M. Froment, J. Bruneaux, *Thin Solid Films* **1997**, *301*, 242 – 248.
[17] A. Kraft, H. Hennig, A. Herbst, K. H. Heckner, *J. Electroanal. Chem.* **1994**, *365*, 191 – 196.
[18] U.S. Geological Survey, *Mineral Commodity Summaries. Copper* **2011**, 48.
[19] C. M. Lieber, Z. L. Wang, *MRS Bull.* **2007**, *32*, 99 – 108.
[20] Y. N. Xia, P. D. Yang, Y. G. Sun, Y. Y. Wu, B. Mayers, B. Gates, Y. D. Yin, F. Kim, Y. Q. Yan, *Adv. Mater.* **2003**, *15*, 353 – 389.
[21] Z. Y. Fan, J. C. Ho, T. Takahashi, R. Yerushalmi, K. Takei, A. C. Ford, Y. L. Chueh, A. Javey, *Adv. Mater.* **2009**, *21*, 3730 – 3743.
[22] A. R. Rathmell, B. J. Wiley, *Adv. Mater.* **2011**, *23*, 4798 – 4803.
[23] A. R. Rathmell, M. Nguyen, M. Chi, B. J. Wiley, *Nano Lett.* **2012**, *12*, 3193 – 3199.
[24] S. M. Bergin, Y.-H. Chen, A. R. Rathmell, P. Charbonneau, Z.-Y. Li, B. J. Wiley, *Nanoscale* **2012**, *4*, 1996 – 2004.
[25] C. D. Wanger, W. M. Riggs, L. E. Davis, J. F. Moulder, G. E. Muilenberg in *Handbook of x-ray photoelectron spectroscopy: a reference book of standard data for use in x-ray photoelectron spectroscopy*, PerkinElmer Corp., Physical Electronics Division, Eden Prairie, Minnesota, USA, **1979**, pp. 80 – 82.
[26] M. C. Biesinger, B. P. Payne, L. W. M. Lau, A. Gerson, R. St. C. Smart, *Surf. Interface Anal.* **2009**, *41*, 324 – 332.